Original Article

Journal of Tissue Engineering
Volume 10: 1–12
© The Author(s) 2019
Article reuse guidelines:
sagepub.com/journals-permissions
DOI: 10.1177/2041731419881528
journals.sagepub.com/home/tej
SAGE

Noninvasive measurement of cell/colony motion using image analysis methods to evaluate the proliferative capacity of oral keratinocytes as a tool for quality control in regenerative medicine

Emi Hoshikawa[1,2], Taisuke Sato[3], Yoshitaka Kimori[4], Ayako Suzuki[1], Kenta Haga[1], Hiroko Kato[1], Koichi Tabeta[2], Daisuke Nanba[5] and Kenji Izumi[1]

Abstract

Image-based cell/colony analyses offer promising solutions to compensate for the lack of quality control (QC) tools for noninvasive monitoring of cultured cells, a regulatory challenge in regenerative medicine. Here, the feasibility of two image analysis algorithms, optical flow and normalised cross-correlation, to noninvasively measure cell/colony motion in human primary oral keratinocytes for screening the proliferative capacity of cells in the early phases of cell culture were examined. We applied our software to movies converted from 96 consecutive time-lapse phase-contrast images of an oral keratinocyte culture. After segmenting the growing colonies, two indices were calculated based on each algorithm. The correlation between each index of the colonies and their proliferative capacity was evaluated. The software was able to assess cell/colony motion noninvasively, and each index reflected the observed cell kinetics. A positive linear correlation was found between cell/colony motion and proliferative capacity, indicating that both algorithms are potential tools for QC.

Keywords

Oral keratinocyte, quality control, regenerative medicine, cell/colony motion, image analysis

Date received: 11 June 2019; accepted: 19 September 2019

Introduction

Recent advances in epidermal and corneal epithelial tissue engineering have led to a state in which tissue defects caused by diseases or injuries can be replaced or repaired using autologous tissues and cells.[1,2] Achieving maximum therapeutic effects depends on the retention of keratinocyte stem cell populations in culture for epidermal and corneal cell sheet grafting. This status should be validated by quality control (QC) during manufacturing in the field of regenerative medicine.[3] In the laboratory, to monitor stem cell maintenance during cell culture, retrospective methods and molecular biological analyses such as quantitative polymerase chain reaction and immunohistochemistry have been employed to assess cellular characteristics at

[1]Division of Biomimetics, Graduate School of Medical and Dental Sciences, Niigata University, Niigata, Japan
[2]Division of Periodontology, Department of Oral Biological Science, Graduate School of Medical and Dental Sciences, Niigata University, Niigata, Japan
[3]Center for Transdisciplinary Research, Institute for Research Promotion, Niigata University, Niigata, Japan
[4]Department of Management and Information Sciences, Faculty of Environmental and Information Sciences, Fukui University of Technology, Fukui, Japan
[5]Department of Stem Cell Biology, Medical Research Institute, Tokyo Medical and Dental University, Tokyo, Japan

Corresponding author:
Kenji Izumi, Division of Biomimetics, Graduate School of Medical and Dental Sciences, Niigata University, 2-5274 Gakkocho-dori, Chuo-ku, Niigata city 951-8514, Japan.
Email: izumik@dent.niigata-u.ac.jp

specific time points. However, because the destructive nature of these methods does not allow real-time and aseptic assessments over time, such methods are not optimal for the QC of cells for therapeutic use. The lack of effective metrics for cell quality, which are noninvasive and produce quantitative parameters, is a significant problem and is an obstacle to the development of quality-assured cellular products for clinical use that are compliant with regulatory requirements.[4] Therefore, expert technicians' manual observation for monitoring cells is still being used as a QC method in facilities that manufacture cellular products; however, such empirical approaches are non-quantitative and require experienced skills.

As a cell source for therapeutic use, oral keratinocytes have been clinically applied to treat corneal and oesophageal lesions in humans using cell sheet engineering and have been used to reconstruct oral mucosa defects using three-dimensional (3D) cellular constructs, such as *ex vivo*-produced oral mucosa equivalents.[5–7] Although oral keratinocytes have not been introduced commercially as biological products, the cell engineering process needs to be compliant with regulatory requirements to ensure the safety and efficacy of engineered cellular products.[8] Because there are no universal guidelines for assessing those products during manufacturing for use in humans, it is necessary for manufacturers to evaluate each product independently on a case-by-case basis to conform to Food and Drug Administration requirements.[9]

Because developing a noninvasive approach for the QC of cultured cells is crucial, the use of image processing to quantitatively analyse information obtained from microscopic images has been attractive for noninvasive cell quality evaluation. Recently, cell morphology-based image analyses and subsequent predictions were successfully applied to mesenchymal stem cells and colonies and to induced pluripotent cells, evaluating individual microscopic images for monitoring cell and colony status.[10–13] For epidermal keratinocytes, the rotational speed of a two-cell colony that is monitored noninvasively using image analysis can be used to predict its proliferative potential at an early stage of cell culture, providing robust evidence that cell motion is correlated with stemness.[14] Thus, it is likely that an oral keratinocyte stem cell population also has a significant proliferative capacity, although this has not been identified due to the lack of specific markers.[15] In contrast, the measurement of rotational speed appears to be difficult to apply to oral keratinocytes because the colonies are less densely packed than those of epidermal keratinocytes due to the feeder layer-free culture system, which is imposed by the selective nature of oral and maxillofacial surgery.[16] There is an apparent need to develop various methods to monitor cell motion specific to oral keratinocytes because there is currently no method available to measure proliferative capacity in a noninvasive manner.

To quantitatively and noninvasively analyse the motion of keratinocyte cells and colonies, we implemented two image analysis algorithms: optical flow (OF) and normalised cross-correlation (NCC). We used two approaches because multiple analyses enhance the reliability and robustness of QC in regenerative medicine. OF refers to the distribution of the apparent motion of brightness patterns between two consecutive frames, caused by the movement of objects.[17] OF produces a two-dimensional (2D) vector field in which each vector is a displacement vector showing the movement of points from the first frame to the second. The vector field provides information about the rate of change of the arrangement of the objects. The similarity in colony morphology between adjacent time frames was also measured using the NCC method.[18] NCC is a simple and effective method of measuring similarity and is robust against variations in image brightness. It has been widely used in image matching and image recognition technology based on computer vision, such as object detection, tracking and stereo matching.[19–22] Although both algorithms have been often applied to the study of cell behaviour and function in basic science, there are few applications of their use in regenerative medicine. To apply each cell motion measurement algorithm as a QC tool, we established two-cell kinetic parameters: mean motion speed (MMS) and mean dynamic index (MDI), based on OF and NCC, respectively. The combination of time-lapse observation of oral keratinocytes and image processing analyses allows the generation of quantitative, noninvasive imaging metrics by recognising and tracing individual cells within colonies.

This study aims to examine the applicability and feasibility of the two basic indices, motion speed (MS) and dynamic index (DI), by applying two algorithms, OF and NCC, to produce a noninvasive and quantitative tool for the evaluation of oral keratinocyte cell and colony motion. We analysed the correlation between the proliferative capacity of oral keratinocytes and the two-cell kinetic parameters, MMS and MDI of the colonies. These cell/colony motion indices have a lot of potential for use in QC of cells in regenerative medicine and pharmacological screening.

Materials and methods

Procurement of oral tissue samples

The protocol for obtaining human oral mucosa tissue samples was approved by the Niigata University Medical & Dental Sciences Hospital Internal Review Board (2015–5018). Patients who underwent minor dentoalveolar surgery were provided with sufficient information regarding this study, and all participating individuals signed an informed consent form.

Primary oral mucosa keratinocyte culture

Primary oral mucosa keratinocyte cultures were established, and cells were serially subcultured as previously described.[23] Briefly, after excess blood on the tissue specimen was removed using a scalpel, the specimen was transferred to a 0.025% trypsin/EDTA solution (Thermo Fisher Scientific, Waltham, MA, USA) containing 1.5% Antibiotic-Antimycotic (Thermo Fisher Scientific) and soaked for approximately 16 h at room temperature. Oral mucosa keratinocytes were mechanically dissociated from the underlying connective tissue in a 0.0125% defined trypsin inhibitor (Thermo Fisher Scientific), resuspended in 'complete' EpiLife® supplemented with EpiLife Defined Growth Supplements (Thermo Fisher Scientific), 0.06 mM Ca^{2+}, plated at a density of 3.0–4.0 $\times$ 10^5 cells in a 35 mm dish (Eppendorf) with complete EpiLife® medium, and fed every other day. Four days after cell plating, the 35 mm dish was subjected to time-lapse observation.

Time-lapse imaging and image processing

Cells grown in the 35 mm dish were imaged using a Keyence BZ-X710 all-in-one fluorescence microscope equipped with a 5% CO_2 and temperature-controlled chamber and time-lapse tracking system (Keyence, Osaka, Japan). Phase-contrast images were acquired at 15 min intervals for 24 h, producing a total of 96 images, using $\times$4 PlanFluor NA0.13 PhL objective lens. The images were converted to video files using a BZ-X analyser (Keyence) (Supplemental material 1 and 2). The video files were analysed using our image analysis software based on the OF and NCC algorithms. Two information scientists blinded to any information about the cells randomly chose colonies.

Principles of the image analyses for quantitative, noninvasive measurement of oral keratinocyte colony motion

(1) Optical flow. OF is an image processing algorithm that can track motion between two consecutive images. OF is a well-studied algorithm in computer vision and is useful for following the movement of objects that possess intricate shapes. It is also advantageous when individual objects, such as cells and/or cell colonies, cannot be identified. Thus, in the life sciences, this technique is useful in the kinematic analysis of living bodies.[24–26] In this study, the cells' motion captured in time-lapse movies was quantified using the OF computation methods. OF analysis was performed using the Farnebäck algorithm,[27] which is based on polynomial expansion. Although the OF algorithm includes the Lucas–Kanade method[28] among others, this study used the Farnebäck method because of its high accuracy compared with other methods. Using this algorithm, the motion was estimated with high accuracy by approximating the intensity of each pixel with a quadratic polynomial and comparing the coefficients between frames.

Let $f_t(\mathbf{r})$ be the intensity of a pixel located at $\mathbf{r}$ in the frame corresponding to time t, then $f_t(\mathbf{r})$ is described as follows

$$f_t(\mathbf{r}) = \mathbf{r}^T \mathbf{A}_t \mathbf{r} + \mathbf{b}_t^T \mathbf{r} + c_t$$

where $\mathbf{r}$ is a position vector indicating the position (x, y), $\mathbf{A}$ is a symmetric matrix, $\mathbf{b}$ is a vector and $\boldsymbol{c_t}$ is a scalar. Expand the above equation

$$\begin{aligned} f_t(\mathbf{r}) &= (x\ y)\begin{pmatrix} p & q \\ q & r \end{pmatrix}\begin{pmatrix} x \\ y \end{pmatrix} + (s\ t)\begin{pmatrix} x \\ y \end{pmatrix} + c_t \\ &= px^2 + 2qxy + ry^2 + sx + ty + c_t \end{aligned}$$

where c_t, p, q, r, s and t are obtained by normalised convolution in the neighbourhood of $\mathbf{r}$. The displacement vector $\mathbf{v}_t$ at $\mathbf{r}$ from the frame t to $t + 1$ is estimated using $f_t(\mathbf{r}) = f_{t+1}(\mathbf{r} + \mathbf{v}_t)$ as follows

$$\mathbf{v}_t = -\frac{1}{2}\mathbf{A}_t^{-1}(\mathbf{b}_{t+1} - \mathbf{b}_t)$$

The displacement vector $\mathbf{v}_t$ indicates how much a position (x, y) in the image has moved from the image in the frame corresponding to time t to the next. To calculate the solution stably, the coefficient $\mathbf{A}_t$ is approximated as follows

$$\bar{\mathbf{A}}_t = \frac{\mathbf{A}_t + \mathbf{A}_{t+1}}{2}$$

Using $\bar{\mathbf{A}}_t$, we obtain

$$\bar{\mathbf{A}}_t \mathbf{v}_t = \Delta\mathbf{b}_t$$

where $\Delta\mathbf{b}_t = (\mathbf{b}_{t+1} - \mathbf{b}_t)/2$. In the Farnebäck algorithm, the energy function over a neighbourhood B of $\mathbf{r}$ is introduced as follows

$$e(\mathbf{v}_t(\mathbf{r})) = \sum_{\Delta\mathbf{r}\in B} w(\Delta\mathbf{r}) \left\| \bar{\mathbf{A}}_t(\mathbf{r} + \Delta\mathbf{r})\mathbf{v}_t(\mathbf{r}) - \Delta\mathbf{b}_t(\mathbf{r} + \Delta\mathbf{r}) \right\|^2$$

where $w(\Delta\mathbf{r})$ becomes a weight function for the points in the neighbourhood B. The displacement vector $\mathbf{v}_t(\mathbf{r})$ is determined to minimise the energy and is obtained using

$$\begin{aligned} \mathbf{v}_t(\mathbf{r}) = &\left(\sum_{\Delta\mathbf{r}\in B} w(\Delta\mathbf{r}) \bar{\mathbf{A}}_t^T(\mathbf{r} + \Delta\mathbf{r}) \bar{\mathbf{A}}_t(\mathbf{r} + \Delta\mathbf{r}) \right)^{-1} \\ &\cdot \sum_{\Delta\mathbf{r}\in B} w(\Delta\mathbf{r}) \bar{\mathbf{A}}_t^T(\mathbf{r} + \Delta\mathbf{r}) \Delta\mathbf{b}_t(\mathbf{r} + \Delta\mathbf{r}) \end{aligned}$$

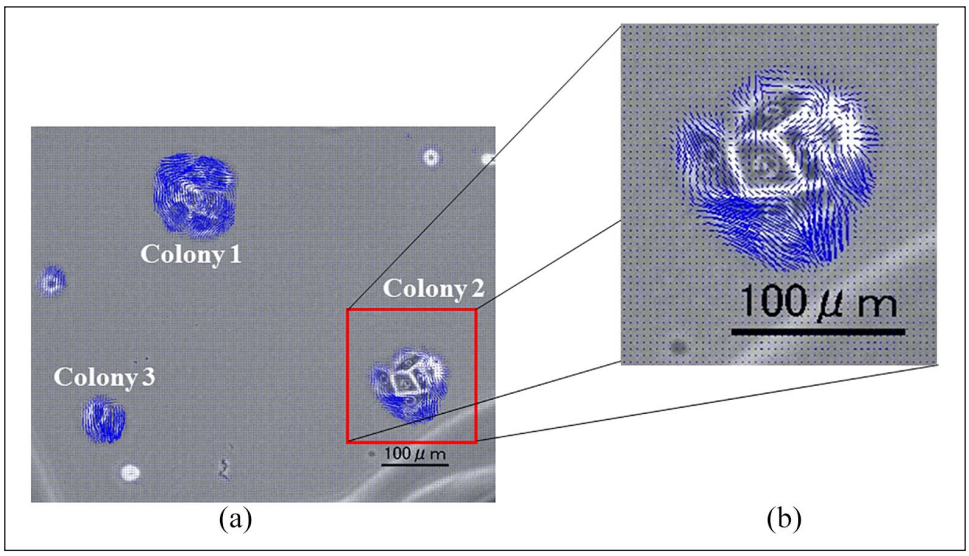

Figure 1. Basic principles of the OF algorithm used to calculate the MS: (a) A representative distribution of the displacement vectors calculated by OF analysis is shown for three extracted colonies, labelled 1, 2 and 3. All three colonies are used for explaining the following methods and results. The original video file is provided in Supplemental material 1 and 2 movies and (b) higher magnification of colony 2, surrounded by a red line in Figure 1(a). The motion speed of colony 2 was determined as the mean value of the magnitude of vectors with values greater than 1 within the region.

The actual displacement vectors are estimated by an iterative operation based on the above equation. The result from this processing is a 2D vector field in which for each pixel in the image, there is a displacement vector $\mathbf{v}_t$.

In this study, we used the highly optimised code (OpenCV library, ver.3.4) to perform calculations using the Farnebäck algorithm. As calculation parameters, the neighbourhood area size was set to 5 × 5 pixels and other parameters used default values. The runtimes are approximately 270 s on a 1920 × 1440 resolution for cell images (96 frames) using a single CPU (core i7-7700K, 4.20 GHz) core on a common desktop PC (memory, 16 GB).

(2) Template matching based on NCC. Template matching based on cross-correlation is a basic statistical approach for image recognition and can evaluate the correspondence between a template image and an input image. It gives a measure of the degree of similarity between the two images. In the present study, NCC[18] was used for template matching. In NCC, the cross-correlation value is calculated by subtracting the average value of the intensity from each calculation region. It has the advantage of not being very susceptible to variations in image brightness and noise. In this study, the target colony region was tracked in all frames, and the motion of cells based on similarity was calculated between neighbouring frame pairs.

Determination of MS of the colony

The Farnebäck algorithm obtained from the OpenCV library gives the displacement vector of each pixel in every two consecutive frames of the video (Figure 1(a)). In Figure 1(a), the displacement vectors are indicated by blue dots. The magnitude of the displacement vector signifies the displacement of motion, and the angle of the vector specifies the direction of the motion, which is called the motion vector. The motion vector at each pixel is drawn on every frame, the displacement of their motion is shown by the magnitude of the motion vectors and their direction is indicated by the angle of the motion vectors. A total of 96 sequence frames were created, in which vectors are drawn on the extracted area of the colony in each image (Figure 1; Supplemental material 3). Pixels with larger movements have larger motion vectors.

In our preliminary experiment, when we calculated the MS ($||\mathbf{v}_t||$) of only the background in which the cell/colony area was not contained, the $||\mathbf{v}_t||$ reached a maximum of 0.57 pixels/frame. In contrast, when we calculated the MS of the cell/colony area, the minimum was 1.12 pixels/frame. Consequently, in this experiment, we defined the area whose MS is equal to or greater than 1.00 pixel/frame as corresponding to a cell/colony area. Therefore, as shown in Figure 1(b), after applying the boxed area surrounded by a red line that contained the extracted colony on the movie file, the mean speed of cells/colony at frame t is calculated as

$$S_t = \frac{1}{N} \sum_{\{\mathbf{r} \in A \| \mathbf{v}_t(\mathbf{r}) \| \geq 1\}}^{N} \left\| \mathbf{v}_t(\mathbf{r}) \right\|$$

where S_t is the mean speed (pixel/frame) at frame t, $\mathbf{v}_t(\mathbf{r})$ is the displacement vector calculated using OF, $\mathbf{r}$ is a position vector and N is the total number of pixels added. Thus, the mean speed of each frame is obtained. However, for further accuracy improvement of S_t, we believe that it is necessary to extract the area of cell/colony for calculation by using another technique such as 'semantic segmentation' and so on.[29] Further system improvement is currently underway.

To convert the number of pixels into the distance that the target cells have moved, we used Image J (National Institutes of Health, Bethesda, MD, USA, http://imagej.nih.gov/ij/). The 100-μm scale bar on the movie was determined to be equal to 53.3333 pixels; the resulting one pixel is identical to 1.875 μm in these images. Moreover, because the interval between the frames in the time-lapse movie is 15 min, the speed per hour (60 min) of the target cells can be calculated by multiplying by 4 (= 60 / 15). As a result, the resulting MS in μm/h was calculated by multiplying S_t by the coefficient of 7.5 (= 1.875 × 4).

Determination of the DI of the colony using the template-matching approach

The motion of the colony-forming cells was also quantitatively measured and evaluated using the DI. DI is calculated using the template-matching approach NCC. The template-matching approach was performed to measure the similarity between the template (the cell colony region in the i-th frame) and overlapping areas in the (i + 1)-th frame. The NCC coefficient (ρ) between the template and the input image at position (x, y) is defined as follows

$$\rho(x,y)=\frac{\sum_{q=0}^{M-1}\sum_{p=0}^{L-1}\left[I(x+p,y+q)-\mu(I'(x,y))\right]\cdot\left[T(p,q)-\mu(T)\right]}{\sqrt{\sum_{q=0}^{M-1}\sum_{p=0}^{L-1}\left[I(x+p,y+q)-\mu(I'(x,y))\right]^2\cdot\sum_{q=0}^{M-1}\sum_{p=0}^{L-1}\left[T(p,q)-\mu(T)\right]^2}}$$

Here, I is the input image, T is a template of size $L \times M$ pixels and $I'(x, y)$ is a partial image of I at position (x, y), and that region coincides with T. The average intensity values in the partial image and the template are given by $\mu(I'(x, y))$ and $\mu(T)$, respectively. These are given as follows

$$\mu(I'(x,y))=\frac{1}{M\times L}\sum_{q=0}^{M-1}\sum_{p=0}^{L-1}I(x+p,y+q)$$

$$\mu(T(p,q))=\frac{1}{M\times L}\sum_{q=0}^{M-1}\sum_{p=0}^{L-1}T(p,q)$$

The position of the maximum coefficient value (ρ_{max}) corresponds to the position of the colony of interest. This position is estimated in each frame, and the coefficient value is used for cell/colony motion analysis.

The proposed template-matching approach is as follows (Figure 2):

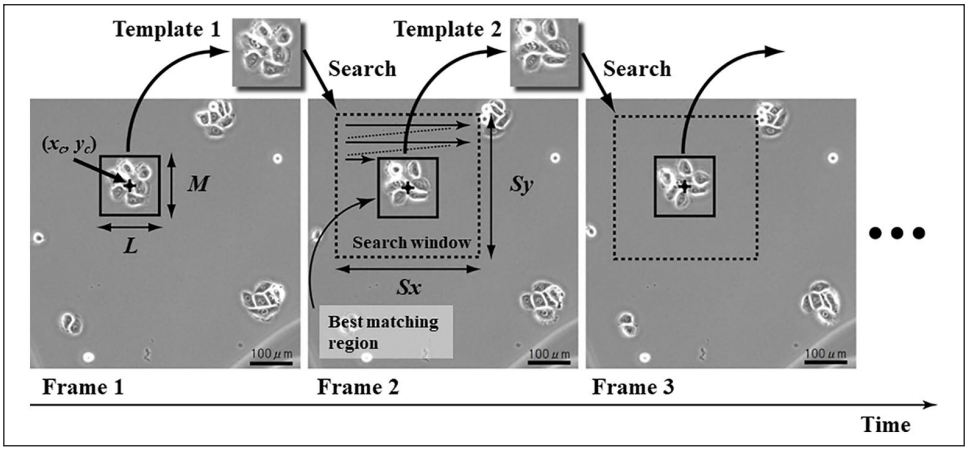

Figure 2. Illustration of the template-matching procedure in the NCC. Basic principle of the NCC algorithm to calculate the normalised cross-correlation coefficient (ρ), which is finally converted into the DI.

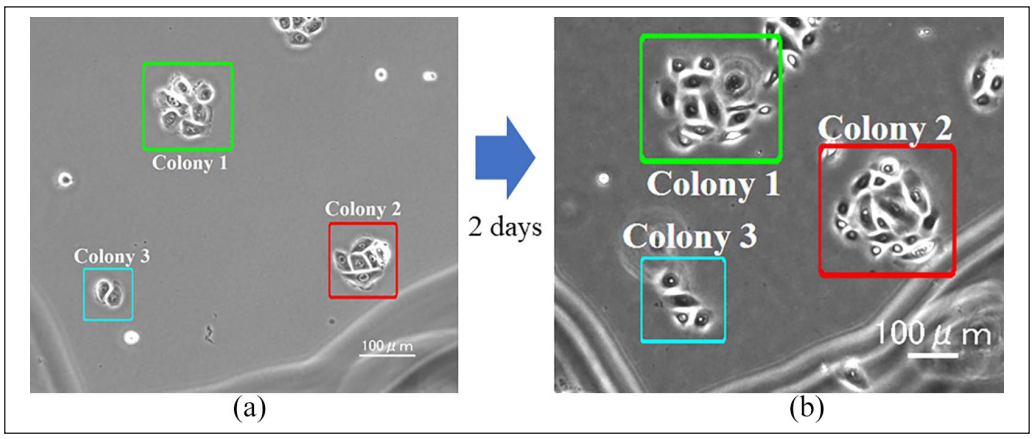

Figure 3. Illustration of the method of determining the proliferative capacity of the extracted colonies: (a) A representative area of the initial image of time-lapse observation, including three extracted colonies that are enclosed with individual boxes, labelled colonies 1, 2 and 3, delineating with lines coloured light green, red and blue. The number of cells is six in colony 1, six in colony 2, and two in colony 3 and (b) the entire image scanned after fixation of the culture dish, identical to Figure 3(a). After 48 h in culture, cells in all colonies proliferated and produced daughter cells, resulting in 13 cells in colony 1, 16 in colony 2, and 4 in colony 3.

1. Marking target colonies: The target colonies to be tracked are extracted manually from the first frame. The colony region is marked, and the centroid of this region (x_c, y_c) is defined as the position of the target colony. The first template is generated by cropping around the centroid.
2. Finding the next template in the second frame: Template matching in the second frame is performed in a search window of size $Sx \times Sy$ pixels around the centroid of the current template. The best-matching region is extracted as the next template.
3. Template updating: Template matching is performed in the third frame using the template from the second frame. The best-matching region in the third frame is extracted as the template for the third frame.
4. Iterating 'Steps 2 and 3' in subsequent frames: Templates of the i-th frame ($i = 2, 3, 4, \ldots, N$) are used as the updated templates for template matching in the next frame.

The extracted cell/colony motion was analysed using this method. The DI computes the difference in the state of colonies between consecutive frames; its value reflects the shape and size of colonies that change over time. The DI of the k-th extracted colony is defined as follows

$$DI_k = \sum_{i=2}^{N} \left(1 - \rho_{max}^{i}\right)$$

where N denotes the total number of frames. The value obtained by averaging the dissimilarities of the k-th colony over all frames represents the motion of the k-th colony. Higher values of this index indicate greater cell/colony motion.

Determination of the proliferative capacity of a targeted colony

Twenty-four hours after the time-lapse imaging was completed, cultured oral keratinocytes in the 35 mm dish were fixed with 10% formalin, resulting in a total of 144 h in culture. The entire surface of the dish was scanned using the Keyence BZ-X700 all-in-one fluorescence microscope. The number of cells comprising each target colony was manually counted in the first image of the time-lapse tracking (Figure 3(a): The number of cells in each colony is six in colony 1, six in colony 2, and two in colony 3) as well as in the entire scanned image (Figure 3(b): The number of cells in each colony is 13 in colony 1, 16 in colony 2, and 4 in colony 3). As a parameter of proliferative capacity, population doublings (PD) were calculated using the following formula[30]

$$PD = \left[\log\left(\frac{N}{N_0}\right)\right]\left[\log 2\right]^{-1}$$

where N = number of cells within the resulted colony and N_0 = number of cells within the initial colony in the first image of the time-lapse tracking.

A step-by-step chart of this experimental design and procedures is shown in Figure 4.

Validation of two algorithms

Furthermore, we validated the OF algorithm used in this study by comparing the MS in three representative colonies with the data obtained by manual tracking of individual cells within each colony. The detailed information is described in Supplemental material 4.

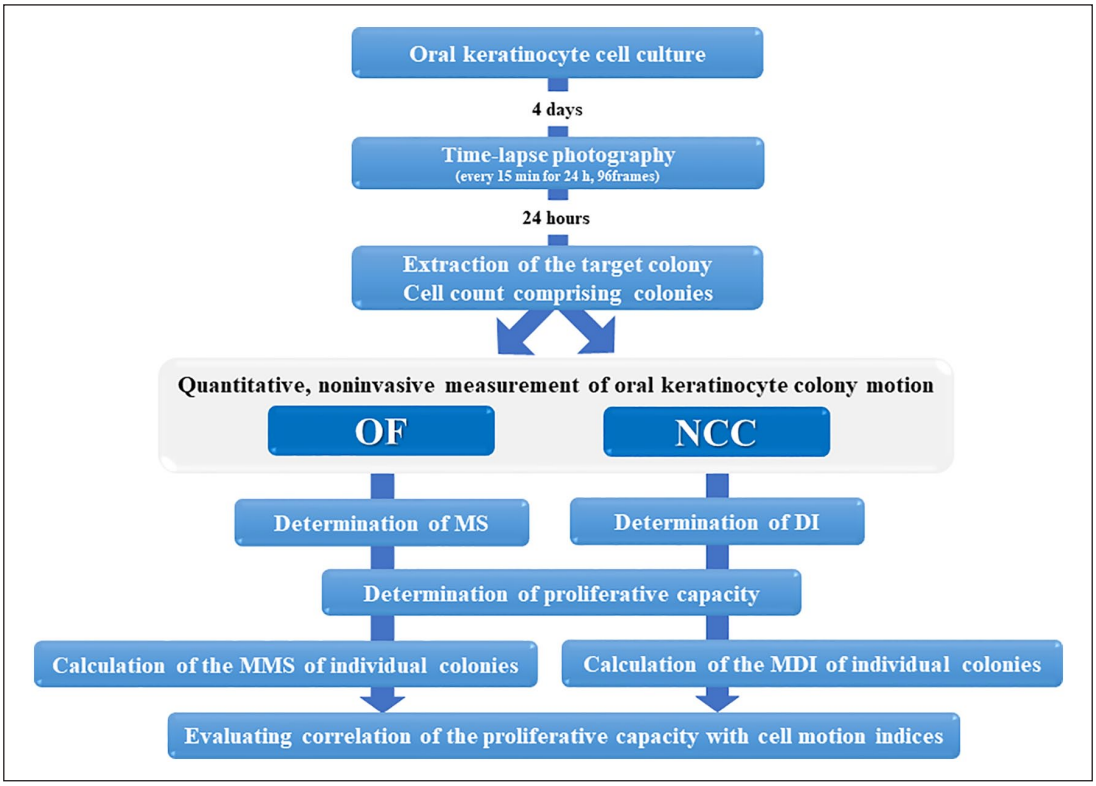

Figure 4. A step-by-step chart of the experimental design and procedures.

Statistical analysis

To examine the strength of a linear association between PD and MMS/PD and MDI, the Pearson correlation coefficient was used, and coefficient, r, and p values were calculated using Excel.

Data availability

The software and datasets generated and analysed during this study can be provided by the corresponding author upon reasonable request due to pending patent application.

Results

Calculation of the MMS and MDI of individual colonies

To implement a quantitative measurement of cell/colony motion, two algorithms were applied to target colonies on the video files. The motion behaviour of individual cells/colonies was successfully quantified, indicating that both indices, MS and DI, can be applicable and feasible for the quantitative measurement of cell/colony motion (Figures 5(a) and (b)). The sum of the MS of the total 96 frames was divided by the 96 results in MMS (μm/hour), producing a representative MS for the target colony. The average of the total 96 DIs was used to produce the MDI, a representative value of a target colony's DI. The MMSs (mean ± standard deviation) of the colony of 1, 2 and 3 were 35.27 ± 10.54, 30.42 ± 8.97 and 27.98 ± 11.64 (μm/hour) and their MDIs (mean ± standard deviation) were 0.58 ± 0.11, 0.54 ± 0.10 and 0.40 ± 0.13, respectively. The ordering of the MMSs of three colonies is the same as that of their MDIs.

Changes in the MS and DI of all three colonies during time-lapse microscopic observation were compared by overlaying with the histograms (Figure 5(c)). Although the two histograms are not comparable, because they are completely different parameters, the changing pattern appears to be similar between the two histograms.

Furthermore, the data obtained by manual tracking of an individual cell within three colonies demonstrated the validation of the OF algorithm used in this study (Supplemental material 4). In addition, it is possible the validation of the NCC algorithm have been achieved based on the finding that DI becomes higher when cells/colonies move faster. Thus, the DI calculated by the NCC algorithm represents an appropriate parameter for evaluating cell/colony motion.

Correlation of the proliferative capacity of oral keratinocyte colonies with MMS and MDI

When the MMS and MDI of all of the colonies were examined and their PDs were plotted on a scatterplot, both

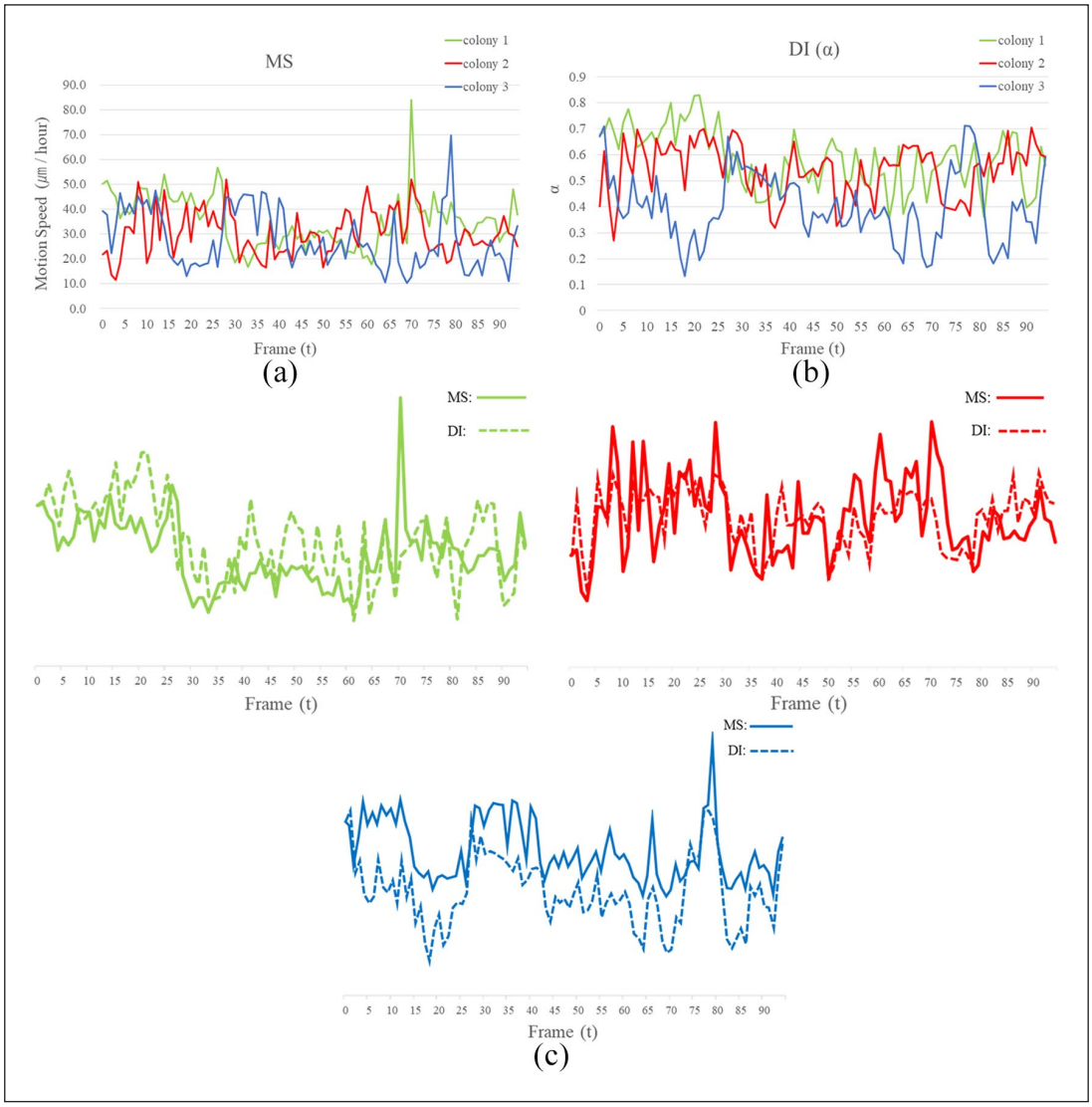

Figure 5. Representative outcomes of MS and DI of colonies 1, 2 and 3 in the 96 frames: (a) Changes in MS of colonies 1, 2 and 3, as shown in Figures 3(a) and (b) during time-lapse microscopic observation; (b) changes of DI of colonies 1, 2 and 3, as shown in Figures 3(a) and (b) during time-lapse microscopic observation; and (c) changes in MS (green, red and blue solid line) are overlaid on those of DI (green, red and blue dotted line) of all three colonies, as shown in Figures 3(a) and (b).

showed low-to-moderate positive linear correlation with PD, which was statistically significant (Figures 6(a) and (b)). Thus, oral keratinocyte cell colonies possessing higher proliferative capacity appeared to have higher MMS and MDI values, implying a higher locomotive ability.

Discussion

The quality of cells for therapeutic use during engineering is increasingly acquiring importance, as the final product needs to maximise safety, efficiency and quality in preclinical and clinical trials.[31] Therefore, the quality of cell therapy products depends on the establishment of a robust QC system for maintaining the consistency of the final product during manufacturing.[9] Image analysis during manufacturing cells has considerable potential to provide a part of the solution of this issue.[32–34] For iPS and mesenchymal stem cells, noninvasive image-based cell quality evaluation has been used to predict and evaluate the performance of cell cultures by using image processing technology with specific morphological parameters to determine the relationships between morphological information and cellular quality.[4,11,12] Recent developments in cell image analyses offer unique opportunities for biological applications, such as the discovery of efficient cell behaviour in response to different cell culture conditions and adaptive experiment control.[35] Although advances in optics and imaging systems facilitate the visualisation of a living cell's dynamic processes using time-lapse microscopy images, there have

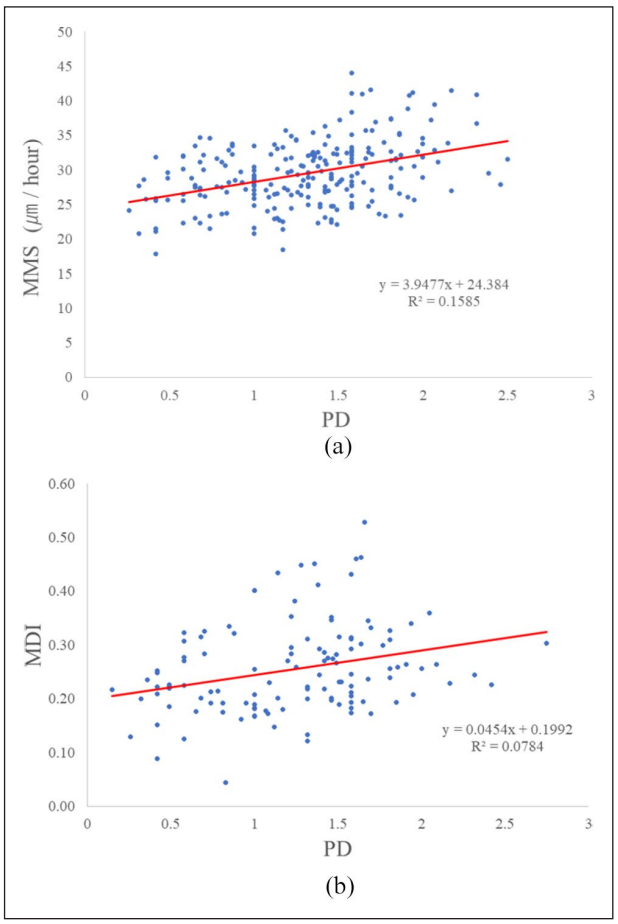

Figure 6. Correlation of the two indices of oral keratinocytes colonies with their proliferative capacity: (a) Scatterplot showing the correlation of MMS between individual colonies and their proliferative capacity (PD). The trend line is shown, and its equation and the correlation coefficient are shown. Pearson's $r = 0.398$, $p = 2.60E\text{-}10$ and $n = 234$ colonies obtained from 13 individuals and (b) scatterplot showing the correlation of MDI between individual colonies and their proliferative capacity (PD). The trend line is shown, and its equation and the correlation coefficient are shown. Pearson's $r = 0.28$, $p = 0.002$ and $n = 120$ colonies obtained from 11 individuals.

been few studies that have evaluated the applicability of these metrics to the cell manufacturing process, especially for epithelial cells.[14] In the present study using oral keratinocytes, for the first time, we applied two algorithms to quantitatively and noninvasively analyse cell/colony motion, producing a label-free tool for the QC of cells in order to produce enhanced biological products.

When we applied the two image analysis algorithms to the time-lapse microscopic video of primary human oral keratinocytes colonies, MS and DI were calculated and determined without any problems, enabling us to noninvasively and quantitatively measure the motion of cells and colonies. This finding suggests that both indices, which are based on the OF and NCC algorithms, can be utilised as potential analytical tools for monitoring complex cell/colony motion. We also found that the cell/colony motion of oral keratinocytes had a low-to-moderate positive linear correlation with their proliferative capacity. Collectively, the image analysis methods used in this study suggested the usefulness of our approach as a noninvasive, quantitative tool for the evaluation of cell/colony motion. Therefore, both MMS and MDI are applicable and feasible for noninvasive monitoring of oral keratinocytes and can potentially be used as tools for QC in regenerative medicine.

This preliminary study also revealed that each algorithm has strengths and weaknesses when measuring cell/colony motion because the purpose of developing the OF algorithm is different from that for NCC algorithm. OF is useful for measuring the movement of objects with complicated structures and contours. However, NCC could categorise the translational motion without any contour changes in the object as no movement. Data accuracy in OF decreases when the object travels a lot. However, template matching, used in NCC, is robust, and the accuracy is not affected in such a case. Nonetheless, as shown in Figure 4(c), the identical order of the two indices obtained from three colonies and the similar outcomes obtained from the two algorithms indicate that each compensates for the limitations of the other, suggesting that the quantitative measurements acquired using two different algorithms collaborate efficiently.[36]

Instead of developing a new technique or approach for specific experimental conditions such as cell migration, an existing technique might allow the analysis or the combination with existing techniques may solve the problem.[37,38] Although OF and NCC are common algorithms for general motion estimation applied to cell cultures, DI calculated by the NCC algorithm represents an original and novel index for evaluating oral keratinocyte cell motion without using speed. Therefore, DI, which is different from MS, is a parameter that permits multifaceted analysis. Because monitoring cells using multiple parameters can ensure a robust QC of cells before transplantation, our strategy may provide a way to use current algorithms more efficiently.[39]

Further improvements and upgrades to the software will be necessary to avoid overestimation in performance for clinical outcomes in future use. For example, oral keratinocytes not only move but also rotate. Our software should be able to capture the rotational motion of cells unless the contours of the cells alter, which is highly unlikely when cells rotate. Nonetheless, the biological significance and mechanisms of the difference in cell motion between rotation and translation have never been elucidated. A weighting for either rotational motion or translational motion may be required in the programme, because epidermal keratinocytes with significant proliferative capacity rotate faster.[14] In addition, OF and NCC did not always capture the dynamics of cell division precisely, because cells shrink and temporarily stop moving while

they divide.[35,40] Further investigations are needed to develop updated software to measure all types of cell motion that allow clinical applications of algorithms. In addition, the molecular mechanisms of cell motion and cellular proliferative capacity need to be investigated.[41–43]

However, the algorithms used in this study have some limitations. A major limitation is that the data we obtained from phase-contrast microscopy were 2D image series, while cell motion is characterised in three dimensions: not only x- and y-axis but also z-axis. Using the current format of both the OF and NCC algorithms, we were unable to analyse the motion towards the z-axis. To enhance the QC of cells in vitro, the ultimate goal is to implement 3D cell motion analysis.[44] Recent studies reported a 3D-imaging system for cell tracking using label-free cells.[45,46] Consequently, wider applications of our algorithms are expected by upgrading the current OF and NCC algorithms that enable calculation of MS and DI in 3D image series acquired from different image modules.

This study demonstrated a positive correlation between cell/colony motions and proliferative capacity at the level of individual colonies consisting of multiple cells, during the initial phase of cell culture. However, as cells proliferate, sampling of distinct colonies will be impossible, due to an increase in cell confluency.[36] Thus, the current protocol is not appropriate to measure the status of the entire cell population. In a clinical setting in which a larger number of cells are present in culture, an alternative protocol is needed to produce a culture vessel-based measurement, instead of a single colony base evaluation, for the later phase of cell culture, in order to eliminate a substandard cell population as a QC. Therefore, our next step will be to explore and validate other noninvasive measurement protocols using MMS and MDI, such as metrics, to evaluate changes in duration, area and timing, in order to determine a proliferating capacity for each culture vessel, an approach which should be more clinically based and realistic for regenerative medicine.

Compared with the remarkable advances in manufacturing of cell and tissue products associated with cell culture technologies, the advances in technologies and methodologies that are informative and efficient for process control obtained by evaluating and analysing the quality of cells for cell-based therapies are lagging behind. Moreover, technologies to measure and evaluate the quality of cells are nascent, and there is a lack of understanding of the current limitations of our technological and methodological abilities to evaluate the quality of cells. These are therefore serious challenges in regenerative medicine. Consistent manufacturing of stable cell/tissue-based products with high quality is required to ensure the consequent outcomes after clinical applications; thus, exploiting information sciences and image-based processing or integrating them with the existing methodologies should be important in regenerative medicine.[47] It is also necessary to develop new analytical tools of quality metrology; however, the choice of parameters of noninvasive assessments needs to be considered, depending on the anticipated performances of the products.[48–50]

Conclusion

In conclusion, in this preliminary study, cell/colony motions of primary human oral keratinocytes were successfully measured in a noninvasive and quantitative manner, using our own software based on two common algorithms, OF and NCC. A positive correlation between the indices of MMS and MDI showing cell/colony motions and their proliferative capacity indicated that these metrics are applicable and feasible to monitor and evaluate cell/colony kinetics during cell culture, demonstrating that MS and DI can be used as tools for QC in regenerative medicine. Our future goal is to incorporate this noninvasive technology into current human clinical protocols, in order to eliminate substandard cell populations prior to transplantation. It is therefore necessary to further determine the criteria of MMS and MDI of substandard cells by examining functional assays of keratinocytes with respect to issues, such as long-term expansion and epithelial regeneration ability.

Acknowledgements

The authors would like to thank Dr. Nobutaka Kitamura for his assistance in performing statistical analysis.

Authorship

E.H., D.N. and K.I. conceived and designed the work. E.H., T.S., Y.K., A.S., K.H., H.K. and K.I. performed the experiments. E.H., T.S., Y.K. and K.I. analysed the data. E.H., T.S., Y.K., A.S., K.H., H.K. and K.T. contributed reagents/materials/analysis tools. E.H., T.S. and K.Y. visualised the data. E.H., T.S., K.Y. and K.I. wrote the original paper. E.H., T.S., Y.K., K.T., D.N. and K.I. reviewed and edited the paper.

Declaration of conflicting interests

The author(s) declared no potential conflicts of interest with respect to the research, authorship and/or publication of this article.

Ethical approval and patient consent

The use of human oral mucosa keratinocytes and the procurement procedure was approved by the Internal Review Board of the Niigata University Medical & Dental Sciences Hospital. Number: 2015-5018, titled ‘Translational research towards advanced regenerative medicine of oral mucosa: From bench to bed side’. Informed consent was obtained from all patients.

Funding

The author(s) disclosed receipt of the following financial support for the research, authorship and/or publication of this

article: This research was supported by JSPS KAKENHI Grant Number 17H04398G to K.I. This work was also supported by JSPS KAKENHI Grant Number JP16H06280, Grant-in-Aid for Scientific Research on Innovative Areas – Platforms for Advanced Technologies and Research Resources 'Advanced Bioimaging Support'.

ORCID iD

Emi Hoshikawa https://orcid.org/0000-0001-7008-7154

Supplemental material

Supplemental material for this article is available online.

References

1. Ronfard V, Rives JM, Neveux Y, et al. Long-term regeneration of human epidermis on third degree burns transplanted with autologous cultured epithelium grown on a fibrin matrix. *Transplantation* 2000; 70(11): 1588–1598.
2. Rama P, Matuska S, Paganoni G, et al. Limbal stem-cell therapy and long-term corneal regeneration. *N Engl J Med* 2010; 363(2): 147–155.
3. Hynds RE, Bonfanti P and Janes SM. Regenerating human epithelia with cultured stem cells: feeder cells, organoids and beyond. *EMBO Mol Med* 2018; 10(2): 139–150.
4. Imai Y, Yoshida K, Matsumoto M, et al. In-process evaluation of culture errors using morphology-based image analysis. *Regen Ther* 2018; 9: 15–23.
5. Nishida K, Yamato M, Hayashida Y, et al. Corneal reconstruction with tissue-engineered cell sheets composed of autologous oral mucosal epithelium. *N Engl J Med* 2004; 351(12): 1187–1196.
6. Ohki T, Yamato M, Murakami D, et al. Treatment of oesophageal ulcerations using endoscopic transplantation of tissue-engineered autologous oral mucosal epithelial cell sheets in a canine model. *Gut* 2006; 55(12): 1704–1710.
7. Izumi K, Feinberg SE, Iida A, et al. Intraoral grafting of an *ex vivo* produced oral mucosa equivalent: a preliminary report. *Int J Oral Maxillofac Surg* 2003; 32(2): 188–197.
8. Sakai D, Schol J, Foldager CB, et al. Regenerative technologies to bed side: evolving the regulatory framework. *J Orthop Translat* 2017; 9: 1–7.
9. Kolkundkar U. Cell therapy manufacturing and quality control: current process and regulatory challenges. *J Stem Cell Res Ther* 2014; 4(9): 1000230.
10. Lo Surdo JL, Millis BA and Bauer SR. Automated microscopy as a quantitative method to measure differences in adipogenic differentiation in preparations of human mesenchymal stromal cells. *Cytotherapy* 2013; 15(12): 1527–1540.
11. Maddah M, Shoukat-Mumtaz U, Nassirpour S, et al. A system for automated, noninvasive, morphology-based evaluation of induced pluripotent stem cell cultures. *J Lab Autom* 2014; 19(5): 454–460.
12. Kerz M, Folarin A, Meleckyte R, et al. A novel automated high-content analysis workflow capturing cell population dynamics from induced pluripotent stem cell live imaging data. *J Biomol Screen* 2016; 21(9): 887–896.
13. Sasaki K, Sasaki H, Takahashi A, et al. Non-invasive quality evaluation of confluent cells by image-based orientation heterogeneity analysis. *J Biosci Bioeng* 2016; 121(2): 227–234.
14. Nanba D, Toki F, Tate S, et al. Cell motion predicts human epidermal stemness. *J Cell Biol* 2015; 209(2): 305–315.
15. Jones KB and Klein OD. Oral epithelial stem cells in tissue maintenance and disease: the first steps in a long journey. *Int J Oral Sci* 2013; 5(3): 121–129.
16. Izumi K, Song J and Feinberg SE. Development of a tissue-engineered human oral mucosa: from the bench to the bed side. *Cells Tissues Organs* 2004; 176(1–3): 134–152.
17. Solem JE. *Programming computer vision with Python*. Sebastopol, CA: O'Reilly Media, 2012, pp. 265–267.
18. Lewis JP. Fast template matching. In: Vision interface, Canadian image processing and pattern recognition society, Québec, QC, Canada, 16–19 May 1995, pp. 120–123.
19. Tsai DM and Lin CT. Fast normalized cross correlation for defect detection. *Pattern Recognit Lett* 2003; 24(15): 2625–2631.
20. Bohs LN and Trahey GE. A novel method for angle independent ultrasonic imaging of blood flow and tissue motion. *IEEE Trans Biomed Eng* 1991; 38(3): 280–286.
21. Zhu K, Xue Y, Fu Q, et al. Hyperspectral light field stereo matching. *IEEE Trans Pattern Anal Mach Intell* 2018; 41(5): 1131–1143.
22. Baydoun M and Al-Alaoui MA. Enhancing stereo matching with classification. *IEEE Access* 2014; 2: 485–499.
23. Kato H, Izumi K, Uenoyama A, et al. Hypoxia induces an undifferentiated phenotype of oral keratinocytes in vitro. *Cells Tissues Organs* 2014; 199(5–6): 393–404.
24. Ronot X, Doisy A and Tracqui P. Quantitative study of dynamic behavior of cell monolayers during in vitro wound healing by optical flow analysis. *Cytometry* 2000; 41(1): 19–30.
25. Boric K, Orio P, Viéville T, et al. Quantitative analysis of cell migration using optical flow. *PLoS ONE* 2013; 8(7): e69574.
26. Tamada A and Igarashi M. Revealing chiral cell motility by 3D Riesz transform-differential interference contrast microscopy and computational kinematic analysis. *Nat Commun* 2017; 8(1): 2194.
27. Farnebäck G. Two-frame motion estimation based on polynomial expansion. In: *Proceedings of 13th Scandinavian conference on image analysis (SCIA), Halmstad*, 29 June–2 July 2003, pp. 363–370. Berlin: Springer.
28. Lucas BD and Kanade T. An iterative image registration technique with an application to stereo vision. In: *Proceedings of 7th international joint conference on artificial intelligence (IJCAI)*, Vancouver, BC, Canada, 24–28 August 1981, pp. 674–679. San Francisco, CA: Kaufmann Publishers.
29. Liu X, Deng Z and Yang Y. Recent progress in semantic image segmentation. *Artif Intell Rev* 2019; 52(2): 1089–1106.
30. Izumi K, Takacs G, Terashi H, et al. Ex vivo development of a composite human oral mucosal equivalent. *J Oral Maxillofac Surg* 1999; 57(5): 571–577.
31. Abdeen AA and Saha K. Manufacturing cell therapies using engineered biomaterials. *Trends Biotechnol* 2017; 35(10): 971–982.

32. Smith D, Glen K and Thomas R. Automated image analysis with the potential for process quality control applications in stem cell maintenance and differentiation. *Biotechnol Prog* 2016; 32(1): 215–223.
33. Zahedi A, On V, Lin SC, et al. Evaluating cell processes, quality, and biomarkers in pluripotent stem cells using video bioinformatics. *PLoS ONE* 2016; 11(2): e0148642.
34. Wakui T, Matsumoto T, Matsubara K, et al. Method for evaluation of human induced pluripotent stem cell quality using image analysis based on the biological morphology of cells. *J Med Imaging* 2017; 4(4): 044003.
35. Kanade T, Yin Z, Bise R, et al. Cell image analysis: algorithms, system and applications. *Proceedings IEEE Workshop on Applications of Computer Vision (WACV)*, Kona, HI, 5–7 January 2011, pp. 374–384. New York: IEEE.
36. Henkel AW, Al-Abdullah LAAD, Al-Qallaf MS, et al. Quantitative determination of cellular-and neurite motility speed in dense cell cultures. *Front Neuroinform* 2019; 13: 15–20.
37. Cordelières FP, Petit V, Kumasaka M, et al. Automated cell tracking and analysis in phase-contrast videos (iTrack4U): development of java software based on combined mean-shift processes. *PLoS ONE* 2013; 8(11): e81266.
38. Masuzzo P, Van Troys M, Ampe C, et al. Taking aim at moving targets in computational cell migration. *Trends Cell Biol* 2016; 26(2): 88–110.
39. Osaki T, Kageyama T, Shimazu Y, et al. Flatbed epi relief-contrast cellular monitoring system for stable cell culture. *Sci Rep* 2017; 7(1): 1897.
40. Czirók A, Varga K, Méhes E, et al. Collective cell streams in epithelial monolayers depend on cell adhesion. *New J Phys* 2013; 15: 075006.
41. Niculiţe CM, Nechifor MT, Urs AO, et al. Keratinocyte motility is affected by UVA radiation – a comparison between normal and dysplastic cells. *Int J Mol Sci* 2018; 19(6): E1700.
42. Friedl P and Mayor R. Tuning collective cell migration by cell-cell junction regulation. *Cold Spring Harb Perspect Biol* 2017; 9(4): a029199.
43. Lång E, Połeć A, Lång A, et al. Coordinated collective migration and asymmetric cell division in confluent human keratinocytes without wounding. *Nat Commun* 2018; 9(1): 3665.
44. Castañeda V, Cerda M, Santibáñez F, et al. Computational methods for analysis of dynamic events in cell migration. *Curr Mol Med* 2014; 14(2): 291–307.
45. Kasprowicz R, Suman R and O'Toole P. Characterising live cell behaviour: traditional label-free and quantitative phase imaging approaches. *Int J Biochem Cell Biol* 2017; 84: 89–95.
46. Sapudom J, Waschke J, Franke K, et al. Quantitative label-free single cell tracking in 3D biomimetic matrices. *Sci Rep* 2017; 7(1): 14135.
47. Uchida S. Image processing and recognition for biological images. *Dev Growth Differ* 2013; 55(4): 523–549.
48. Kuo S, Zhou Y, Kim HM, et al. Biochemical indicators of implantation success of tissue-engineered oral mucosa. *J Dent Res* 2015; 94(1): 78–84.
49. Chen LC, Lloyd WR, Kuo S, et al. The potential of label-free nonlinear optical molecular microscopy to non-invasively characterize the viability of engineered human tissue constructs. *Biomaterials* 2014; 35(25): 6667–6676.
50. Nakagawa K and Kishimoto T. Unlabeled image analysis-based cell viability assay with intracellular movement monitoring. *Biotechniques* 2019; 66(3): 128–133.